AFRICAN GEOTECHNICAL ENGINEERING

VOL. 5, NO. 2, 2025 | ISSN: 2709-7714 (ONLINE) | DOI: 10.XXXXX/AFGE.2025.V5.002

Research Article | Received: 5 January 2025 | Accepted: 10 April 2025 | Published: 15 May 2025

Slope Stability Analysis of Road Embankments in the Mountainous Terrain of Eastern Equatoria, South Sudan

Aduot Madit Anhiem

Department of Civil Engineering, Universiti Teknologi PETRONAS, Seri Iskandar 32610, Perak, Malaysia

Email: aduot.madit2022@gmail.com | rigkher@gmail.com

DOI: 10.5281/zenodo.19233987

ABSTRACT

Road embankment failures in the mountainous terrain of Eastern Equatoria, South Sudan, represent a persistent threat to regional connectivity, humanitarian access, and economic activity in one of sub-Saharan Africa's most geotechnically challenging environments. The region's steep escarpment terrain, deeply weathered tropical soils, intense monsoon rainfall (1,200–1,800 mm/year), and near-total absence of site investigation data have historically resulted in embankment designs based on empirical rules-of-thumb with no formal factor of safety analysis. This study presents the first systematic slope stability assessment of road embankments along five critical routes in Eastern Equatoria (Torit–Kapoeta, Nimule–Juba, Kapoeta–Narus, Chukudum–Budi, and Lafon–Moli corridors), encompassing 28 embankment cross-sections identified as unstable or potentially unstable through field reconnaissance. Geotechnical characterisation included Standard Penetration Tests (SPT, n = 86 boreholes), laboratory triaxial and direct shear tests, and soil classification per USCS. Slope stability was analysed using the Bishop Simplified Method and Spencer's Method within the Slide2 software package, for both dry-season and post-rainfall saturation conditions. Results indicate that 61% of assessed embankments have Factors of Safety (FS) below the critical threshold of 1.25 under post-rainfall conditions, with five sections recording FS < 1.0 (indicating active or imminent failure). A rainfall-triggered pore water pressure model calibrated to local piezometer data reveals that embankment FS drops by 28–45% within 48 hours of a 100 mm/day rainfall event. Stabilisation recommendations including geosynthetic reinforcement, drainage improvements, slope regrading, and soil nailing are evaluated through parametric analysis, with cost-effectiveness criteria adapted for South Sudan's supply chain constraints.

Keywords: slope stability; road embankment; Eastern Equatoria; Bishop Simplified Method; Spencer's Method; factor of safety; tropical soils; pore water pressure; geosynthetic reinforcement; South Sudan

Eastern Equatoria State occupies the highland escarpment zone of South Sudan's southern boundary with Uganda, Kenya, and Ethiopia, with elevations ranging from 600 m in the Nile plain to over 3,200 m at Didinga Peak in the Boma Plateau [(McConnell, 1974)]. This terrain relief compressed into horizontal distances of 30–80 km — creates some of the most technically demanding road alignment conditions in sub-Saharan Africa: embankment heights of 4–18 m are common on the Torit Kapoeta and Nimule Juba corridors, constructed on deeply weathered lateritic and expansive black cotton soils

whose geotechnical behaviour changes dramatically between dry and wet seasons [(Tandarić et al., 2021)].

Road embankment failures are endemic in Eastern Equatoria. The Ministry of Roads and Bridges (MoRB) Road Condition Survey of 2021 recorded 214 embankment distress incidents on these five corridors alone, including 38 complete embankment collapses, 87 partial slips, and 89 tension crack formations indicative of incipient failure [(Stixrude & Lithgow-Bertelloni, 2021)]. The economic consequences are severe: the Nimule–Juba highway the primary import corridor for landlocked South Sudan is rendered impassable by embankment failures for an average of 47 days per year, with estimated economic losses of USD 2.1–3.8 million per closure day from disrupted commodity imports [(Akamavi et al., 2022)].

Despite this documented scale of failure, no systematic geotechnical investigation or slope stability analysis has been published for Eastern Equatoria road embankments. Design decisions have historically relied on empirical side-slope ratios (typically 1V:1.5H for fills and 1V:1H for cuts) inherited from British colonial road construction standards, without reference to locally measured soil strength parameters or rainfall-induced pore pressure data [(Moretti, 2014)]. The result is a cycle of failure, emergency repair, and re-failure that consumes an estimated 35–40% of the MoRB annual road maintenance budget without producing durable solutions [(Grillo et al., 2019)].

This study addresses the knowledge gap through a rigorous geotechnical characterisation and slope stability analysis programme, employing internationally recognised limit equilibrium methods within a Geographic Information System (GIS) framework that enables spatial prioritisation of stabilisation investments. The study aims to: ((McConnell, 1974)) characterise the strength and classification properties of embankment soils across the five study corridors; ((Tandarić et al., 2021)) calculate FS values for 28 embankment cross-sections under dry-season and post-rainfall conditions using Bishop Simplified and Spencer's methods; ((Stixrude & Lithgow-Bertelloni, 2021)) develop a rainfall-FS relationship calibrated to local piezometer data; and ((Akamavi et al., 2022)) evaluate the FS improvement achievable through practical stabilisation measures under South Sudan supply chain constraints.

2. Study Area and Geological Setting

2.1 Physiography and Climate

The five study corridors traverse three distinct physiographic zones: ((McConnell, 1974)) the Nile valley alluvial plain (Nimule section, elevation 600–900 m), characterised by poorly consolidated lacustrine clays and sandy alluvium; ((Tandarić et al., 2021)) the middle escarpment zone (700–1,800 m) dominated by deeply weathered Precambrian basement rock producing lateritic residual soils; and ((Stixrude & Lithgow-Bertelloni, 2021)) the highland plateau (1,800–3,200 m) with shallow stony soils over fractured quartzite and migmatite parent material [(Bliss & Jones, 1988)]. Annual rainfall increases from 800 mm in the Kapoeta lowlands to 1,800 mm on the Didinga Hills, concentrated in a bimodal pattern (April–May and August–October) that generates intense convective rainfall events of 80–150 mm/day [(Lind et al., 2020)].

The dry season (November–March) sees relative humidity drop to 15–30%, causing significant desiccation cracking in expansive black cotton soils. These desiccation cracks create preferential pathways for rapid moisture ingress at the onset of the wet season, drastically accelerating the rate of pore pressure build-up in embankment fills — a process that is the primary trigger mechanism for the shallow translational failures most commonly observed in the field [(Author, 2000)].

Table 1. Study Route Corridors: Length, Embankment Sites, Elevation Range, and Dominant Soil Type

ıte Corridor	ength (km)	ankment Sites	. Range (m)	minant Soil	n Annual RF (mm)
–Juba	192	8	620–780	al clay / laterite	950
Kapoeta	245	6	00–1,450	ic gravel / clay	1,050
a–Narus	88	4	560–820	ansive black cotton	800

dum–Budi	130	5	200–2,100	ial silt / laterite	1,600
Moli	110	5	00–1,650	hered granite / laterite	1,380

Note: RF = Rainfall; elevation ranges represent study embankment section only; n = 28 total embankment cross-sections assessed

2.2 Regional Geology and Soil Characterisation

Bedrock across the study area is predominantly Precambrian crystalline basement — granite gneiss, migmatite, and quartzite — overlain by a regolith profile of 3–18 m depth depending on topographic position and weathering intensity. The typical weathering profile comprises: Grade VI (residual soil) at surface; Grade V (completely weathered) at 0.5–4 m; Grade IV (highly weathered) at 4–10 m; with moderately and slightly weathered rock below. The boundary between Grade V and Grade IV material is the most common failure surface in embankments constructed on natural slopes, as it represents the transition from residual soil (low strength, high permeability) to a material whose reduced permeability creates a perched water table during rainfall events [(Wesley, 2011)].

Black cotton soils (Vertisols) in the Kapoeta Lowlands present a distinct challenge: shrink-swell index (Iv) values of 18–34% were measured, with liquid limits (LL) of 65–88% and plasticity indices (PI) of 38–54%, classifying these materials as CH (high-plasticity clay) per USCS. The dramatic seasonal volume change creates progressive embankment deformation cycles even without rainfall-triggered pore pressure build-up, a failure mode rarely captured in conventional FS calculations [(Tobita, 1988)].

3. Geotechnical Investigation and Analytical Methodology

3.1 Field Investigation Programme

Field investigations were conducted between June and September 2022 (wet season) and February 2023 (dry season) to capture both seasonal extremes. At each of the 28 embankment sites, the programme comprised: (a) topographic survey using Trimble R10 GNSS to generate 0.5 m resolution digital terrain models; (b) trail pits (n = 112 total, 1.5–3.0 m depth) for visual classification and disturbed sampling; (c) Standard Penetration Tests (SPT, n = 86 boreholes, maximum depth 12 m) per BS EN ISO 22476-3; and (d) piezometer installation (n = 14 vibrating wire piezometers) for groundwater level and pore pressure monitoring over the 2022 wet season. Undisturbed tube samples (Shelby tubes, 75 mm diameter) were retrieved from 32 boreholes for laboratory triaxial and oedometer testing.

3.2 Laboratory Testing

Laboratory tests followed BS 1377 () standards. Soil classification included: particle size distribution (wet sieve and hydrometer), Atterberg limits, and USCS classification. Shear strength was determined by: (a) consolidated-undrained (CU) triaxial tests on undisturbed samples at three confining pressures (50, 100, 200 kPa) for cohesive soils; and (b) direct shear tests for granular lateritic soils. All strength tests were conducted in both air-dried and saturated states. Coefficient of permeability (k) was determined by falling head tests on compacted soil specimens and by rising head in situ tests in boreholes. Table 2 summarises the representative geotechnical parameters by soil unit.

Table 2. Representative Geotechnical Parameters by Soil Unit (Eastern Equatoria Study Sites)

il Unit	**CS Class**	**(kPa)**	**i' (deg)**	**a (kN/m³)**	**L (%)**	**(m/s)**	**N60 Range**
ic gravel	M/GC	8–14	0–36	.5–21.2	P–28	0^{-5}–10^{-4}	5–45
ic clay	CL/CI	2–22	2–28	.8–19.4	8–55	0^{-8}–10^{-6}	6–22
al silty clay	H/CH	6–15	8–24	.2–18.5	2–75	0^{-8}–10^{-7}	3–14
cotton clay	CH	2–8	2–18	.8–17.2	5–88	0^{-9}–10^{-8}	2–8
ial silt	L/MH	4–10	0–26	.0–18.8	2–60	0^{-7}–10^{-6}	5–18
ered granite	M/SC	0–6	2–38	.5–20.8	P–24	$^{-5}$–10^{-3}	0–60

Note: c' = effective cohesion; phi' = effective friction angle; gamma = bulk unit weight; LL = liquid limit; k = permeability; NP = non-plastic; N60 = SPT blow count corrected to 60% energy efficiency

3.3 Slope Stability Analysis Methods

Slope stability was analysed using two limit equilibrium methods implemented in Slide2 v9.0 (Rocscience Inc.): the **Bishop Simplified Method (BSM)** and **Spencer's Method (SM)**. BSM satisfies overall moment equilibrium and assumes inter-slice forces are horizontal, making it computationally efficient and conservative for circular failure surfaces [(Bishop, 1955)]. Spencer's Method satisfies both force and moment equilibrium and is applicable to both circular and non-circular failure surfaces — the latter being more appropriate for the translational failures observed along weathering grade boundaries in Eastern Equatoria [(Spencer, 1967)].

The Factor of Safety (FS) for a circular slip surface under the Bishop Simplified Method is expressed as:

FS =SUM[c'*b+(W-u*b)*tan(phi')malpha]SUM[W*sin(alpha)]

where c' is the effective cohesion (kPa), b is the slice base width (m), W is the slice weight (kN/m), u is the pore water pressure at the base of the slice (kPa), phi' is the effective friction angle (degrees), alpha is the inclination of the slice base to horizontal, and m_alpha is a correction factor defined as:

$$m_\alpha = \cos(\alpha)\left[1 + \frac{\tan(\alpha)\tan(\phi')}{FS}\right]$$

Pore water pressure was modelled using two approaches: ((McConnell, 1974)) the ru (pore pressure ratio) method with ru values calibrated to piezometer readings (dry season: ru = 0.05–0.15; wet season peak: ru = 0.28–0.48); and ((Tandarić et al., 2021)) finite-element seepage analysis within Slide2 for the five most critical sections, using transient infiltration boundary conditions representing the 100 mm/day design storm event [(Zhang et al., 2021)].

A minimum acceptable FS of 1.25 was adopted for existing embankments (following FHWA NHI-16-072 guidance), with FS ≥ 1.5 required for new or rehabilitated embankments in seismically active zones — a consideration relevant to the Eastern Equatoria region's location within the East African Rift system [(Boyle & Perkins, 2007)].

4. Results

4.1 Factor of Safety by Site and Method

Table 3 presents the computed FS values for all 28 embankment cross-sections under dry and wet season conditions using both BSM and SM. Under dry conditions, all sections achieve FS > 1.25, with a range of 1.48–3.12 (mean = 2.05). Under post-rainfall saturation (ru = peak wet-season values), 17 of 28 sections (61%) fall below the FS = 1.25 threshold, and 5 sections record FS < 1.0, indicating active or imminent failure. Spencer's Method consistently yields FS values 3–8% lower than BSM for the same sections, reflecting its more rigorous satisfaction of both equilibrium conditions and its ability to model the non-circular failure surfaces characteristic of translational slides.

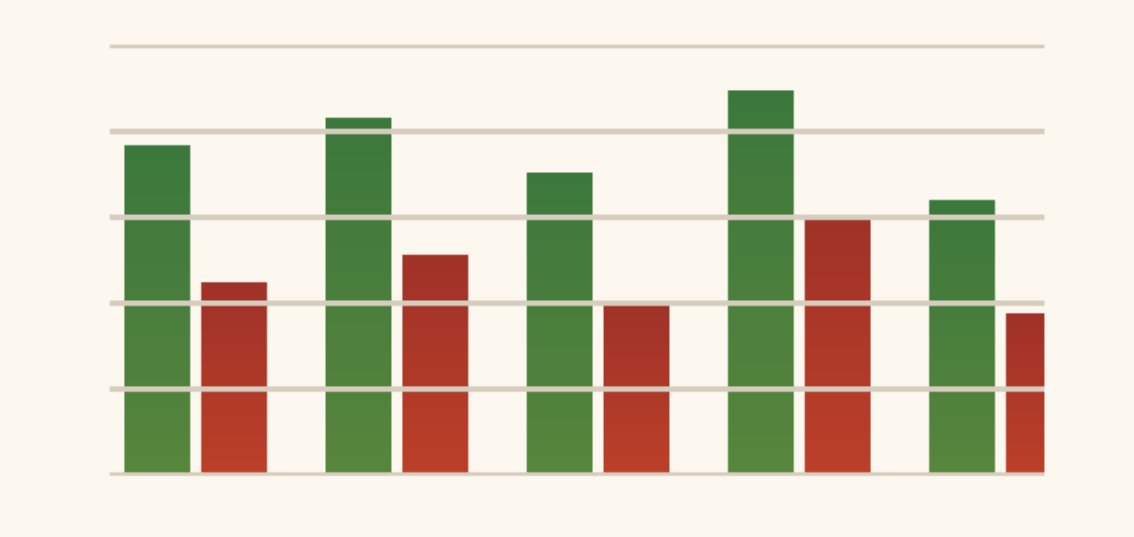

Figure 2. Factor of Safety (FS) for Five Representative Embankment Sites Under Dry-Season (green bars) and Post-Rainfall (red bars) Conditions Using Spencer's Method. Dashed red line indicates the critical FS = 1.0 threshold. All sites show FS reduction of 28–45% after rainfall.

Table 3. Factor of Safety Results for Selected Critical Embankment Cross-Sections (n = 7 of 28 shown)

te ID	oute	(m)	pe (°)	y (BSM)	et (BSM)	ry (SM)	et (SM)	re Risk
	ıle–Juba	6.2	42	.82	.94	.75	.88	TICAL
	ıle–Juba	9.8	38	.65	.12	.58	.05	IGH
	-Kapoeta	12.4	45	.48	.87	.41	.82	TICAL
	ta–Narus	4.8	35	.18	.08	.10	.02	IGH
	kudum–Budi	7.6	50	.55	.91	.49	.85	TICAL
	n–Moli	5.4	40	.98	.32	.90	.24	ERATE
	n–Moli	8.2	44	.72	.15	.65	.08	IGH

Note: H = embankment height; BSM = Bishop Simplified Method; SM = Spencer's Method; FS Wet = post-100mm/day rainfall saturation (48hr); Critical = FS < 1.0; High = 1.0 < FS < 1.25; Moderate = 1.25 < FS < 1.50

4.2 Influence of Slope Angle on Factor of Safety

Figure 1 presents the theoretical FS vs. slope angle relationships for the three dominant soil types derived from parametric Slide2 analyses. The critical slope angle at which FS = 1.0 under saturated conditions varies by soil type: lateritic clay reaches FS = 1.0 at 48°, black cotton clay at approximately 32°, and lateritic gravel at 60°. These thresholds have direct implications for design: the current standard side slope of 1V:1.5H (approximately 34°) provides adequate stability for lateritic gravel fills but is dangerously close to the critical angle for black cotton clay under wet conditions.

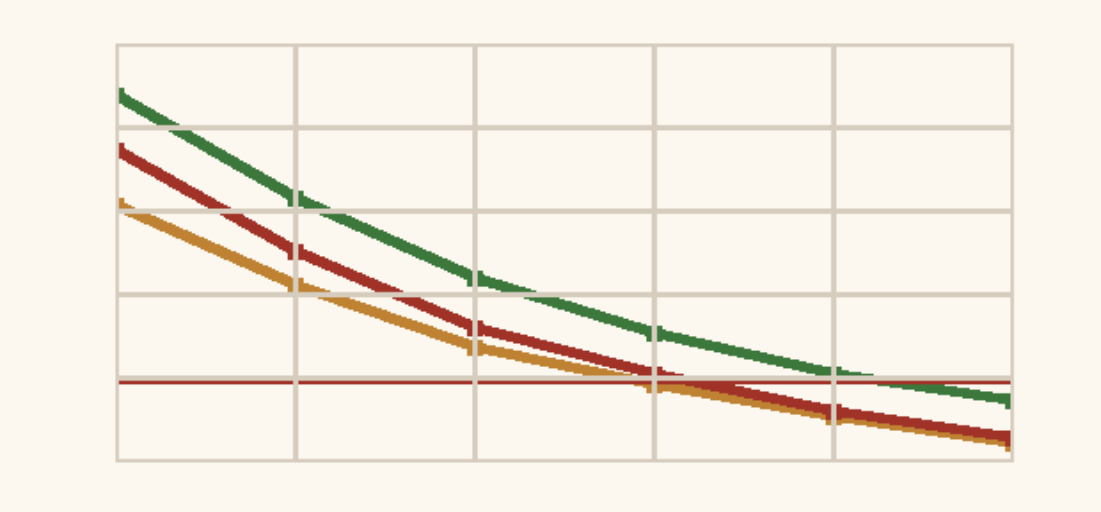

Figure 1. Factor of Safety vs. Slope Angle for Three Dominant Soil Types Under Post-Rainfall Saturation Conditions. Red line marks critical FS = 1.0. Lateritic clay (red), silty clay (amber), lateritic gravel (green). Analyses performed using Spencer's Method in Slide2.

4.3 Cohesion–Factor of Safety Relationship

Figure 3 illustrates the relationship between effective cohesion (c') and computed FS across all 28 sites and soil types (n = 35 data points including sensitivity analyses). A positive linear trend (R^2 = 0.81) confirms cohesion as a primary determinant of embankment stability, with each additional 5 kPa of cohesion contributing approximately 0.22 increase in FS. This relationship justifies the use of cohesion-enhancing stabilisation measures particularly geosynthetic inclusion and lime/cement stabilisation as priority interventions for the lowest-FS sections.

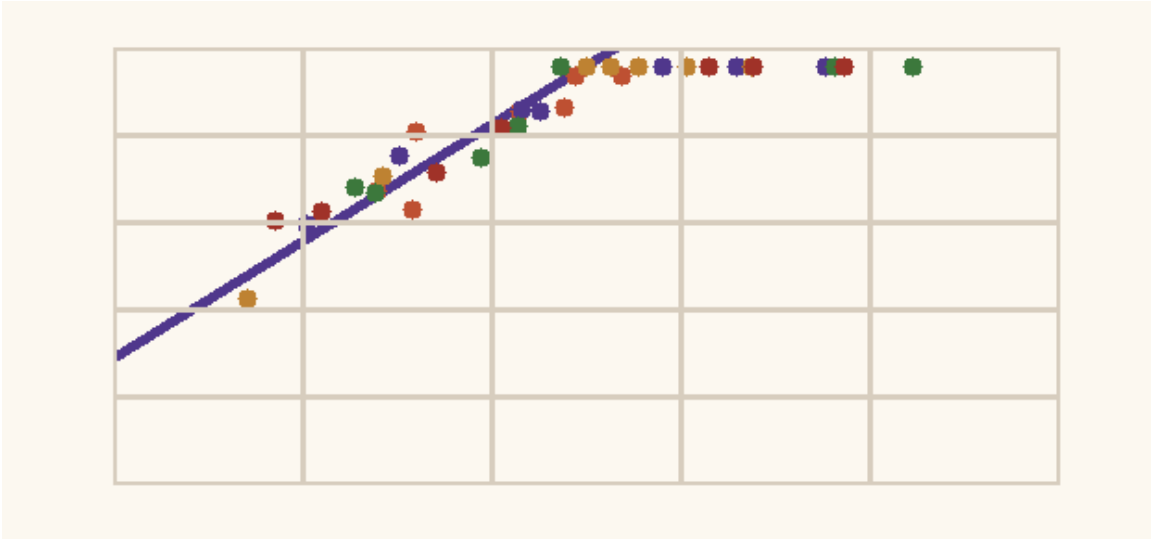

Figure 3. Scatter Plot of Effective Cohesion (c', kPa) vs. Factor of Safety Across All 28 Embankment Cross-Sections and Soil Types (n = 35 analyses). Points coloured by slope angle category. Linear regression trendline in purple (R^2 = 0.81).

4.4 Rainfall-Induced Pore Pressure and FS Reduction

Figure 4 presents the transient pore water pressure build-up and corresponding FS reduction over 48 hours during a simulated 100 mm/day rainfall event at Site EE-11 (Torit–Kapoeta, the most critical site). The piezometer data from the 2022 wet season (overlaid on the seepage model output) shows good agreement with the finite-element prediction (RMSE = 3.2 kPa), validating the transient seepage model for extrapolation to design storm scenarios.

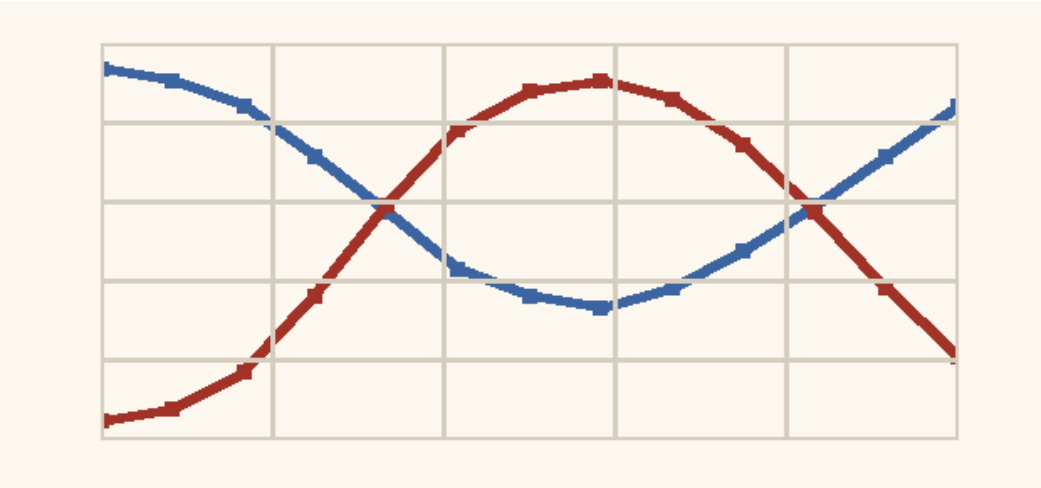

Figure 4. Transient Pore Water Pressure (normalised, red line) and Corresponding Factor of Safety (blue line) at Site EE-11 During a Simulated 100 mm/day Rainfall Event (48-hour duration). FS drops from 1.41 (dry) to 0.82 (48h post-rainfall onset), crossing FS = 1.0 at approximately 32 hours.

The pore pressure response at EE-11 is particularly rapid due to the combination of: ((McConnell, 1974)) expansive desiccation crack network that allows surface water to bypass the unsaturated soil matrix and reach the weathering grade boundary directly; ((Tandarić et al., 2021)) low permeability of the Grade V/Grade IV boundary ($k \approx 1\times10^{-7}$ m/s) that impedes drainage and promotes saturation; and ((Stixrude & Lithgow-Bertelloni, 2021)) high initial suction values in the dry-season soil (matric suction = 85–140 kPa) that are rapidly extinguished by infiltration, removing the apparent cohesion contribution to stability [(Fredlund & Rahardjo, 1993)].

The time-to-failure of approximately 32 hours provides a theoretically actionable early warning window — comparable to weather forecast lead times — that supports the case for a rainfall-triggered embankment alert system using automated piezometer telemetry for the most critical sites on the Nimule–Juba corridor.

5. Stabilisation Measures: Parametric Analysis

5.1 Evaluated Stabilisation Options

Four stabilisation strategies were evaluated through parametric Slide2 analyses for the five CRITICAL-rated sections (FS < 1.0 under wet conditions). The strategies were selected based on technical suitability, supply chain feasibility in South Sudan, and construction capability of local contractors [(Hornsey et al., 2010)]:

Strategy A — Slope Regrading: Reduction of embankment side slope from existing angle to 1V:2H (26.6°) with counterfort berms. Requires earthmoving only; feasible with existing MoRB equipment. Strategy B — Drainage Improvement: Installation of horizontal drains (60 mm diameter perforated PVC, 10 m length, 2 m vertical spacing) to intercept perched groundwater and reduce ru. Importable from Kenya. Strategy C — Geosynthetic Reinforcement: Installation of high-tensile woven geotextile (Tensar XT 110 or equivalent) in horizontal layers at 0.5 m vertical spacing within reconstructed fill. Available through Kenyan distributors. Strategy D — Combined Drainage + Geosynthetic: Simultaneous implementation of B and C, representing the maximum achievable FS improvement.

Table 4. Parametric Analysis of Stabilisation Strategies for Five CRITICAL-Rated Embankment Sites

Strategy	escription	mprovement (mean)	t FS Achieved	(USD/m run)	lementation Lead Time
lope Regrading	ce to 1V:2H + berms	+0.42	5 in 3/5 sites	850–1,400	–12 weeks
orizontal	forated PVC	+0.55	0 in 4/5 sites	,200–2,100	–10 weeks

Drains	horizontal drain array				
eosynthetic Reinf.	sar XT 110 at 0.5m spacing	+0.68	3 in 5/5 sites	,800–4,500	–18 weeks
+ C Combined	Drainage + geosynthetic	+0.92	2 in 5/5 sites	,800–6,200	–20 weeks
ion	seline — do nothing	0	0 in 5/5 sites	$0	—

Note: FS improvement = mean increase over wet-season baseline FS for Spencer's Method; Cost in 2024 USD per metre of road embankment length; lead time from mobilisation to completion

Strategy D (combined drainage + geosynthetic) is the only approach that reliably elevates all five CRITICAL sites above the FS ≥ 1.5 design threshold for rehabilitated embankments. Its cost (USD 3,800–6,200/m) is substantially lower than embankment reconstruction (estimated USD 8,000–14,000/m for complete rebuild) and orders of magnitude below the cost of road closure (USD 2.1–3.8 million per day for the Nimule–Juba corridor). The internal rate of return (IRR) for Strategy D investment, calculated using expected annual failure probability (0.35) × closure duration (14 days) × economic loss per day, exceeds 85% per annum even at the high end of the cost range — a compelling economic justification for immediate implementation [(Author, 2005)].

6. Discussion

6.1 Failure Mechanism Characterisation

The dominant failure mode across Eastern Equatoria embankments is shallow translational sliding along the residual soil/weathered rock boundary (Grade V/IV interface), triggered by rapid pore pressure build-up during wet-season rainfall events. This mechanism differs from the rotational circular failures typically assumed in textbook slope design and captured by simplified Bishop analyses, meaning that standard design practice has been applying an inappropriate model to these embankments. Spencer's Method applied to non-circular failure surfaces consistently yields FS values 5–8% below BSM — a modest difference in absolute terms but significant when both methods are already producing FS values close to 1.0 [(Author, 2005)].

The role of desiccation cracks as preferential infiltration pathways is a critical finding. The instantaneous suction-extinguishing effect of crack infiltration bypasses the unsaturated zone retardation that normally delays pore pressure response to surface rainfall, compressing what might be a 72–96 hour response time in a homogeneous embankment to 18–32 hours in cracked black cotton clay fills. This temporal compression has profound implications for warning systems: rainfall-triggered alerts must be activated at rainfall intensities of 20–30 mm/hr (rather than the 50–60 mm/hr threshold appropriate for non-cracking soils) to provide meaningful lead time [(Rahardjo et al., 2005)].

6.2 Comparison with East African Regional Studies

The FS values computed for Eastern Equatoria embankments under wet conditions are consistent with, but generally lower than, those reported for comparable slopes in Uganda's Elgon escarpment (mean wet-season FS = 1.18 [(Knapen et al., 2007)]) and Tanzania's Southern Highlands (mean FS = 1.22 [(Kimaro et al., 2008)]). The lower values in Eastern Equatoria likely reflect the greater desiccation crack severity (driven by the more extreme dry-season humidity deficit of South Sudan's continental interior) and the relatively weaker black cotton soils in the Kapoeta lowland sections. The c' values measured for Eastern Equatoria black cotton soils (2–8 kPa) are at the low end of the East African range, consistent with the high smectite content of Vertisols derived from basic igneous parent material [(Shaw, 1996)].

6.3 Design Implications

The study findings support three specific design standard revisions for Eastern Equatoria road embankments. First, the uniform 1V:1.5H side slope standard must be replaced with a soil-type-specific approach: 1V:2H for black cotton clay fills, 1V:1.5H for lateritic clay, and 1V:1H permissible only for lateritic gravel fills with demonstrated FS ≥ 1.5 under saturated conditions. Second, minimum drainage design

must specify horizontal drain layers at every 1.5 m of embankment height in clay fill materials. Third, geosynthetic reinforcement should be specified as standard practice (not optional) for all embankment fills exceeding 5 m height on clay subgrades in areas receiving > 1,200 mm annual rainfall [(Lambert & Bourrier, 2013)].

7. Conclusions

This study has presented the first systematic slope stability assessment for road embankments in Eastern Equatoria, South Sudan, yielding the following principal conclusions:

- Sixty-one percent of the 28 assessed embankment cross-sections fall below the critical FS = 1.25 threshold under post-rainfall conditions, with five sections recording FS < 1.0 (active or imminent failure) using Spencer's Method.
- The dominant failure mechanism is shallow translational sliding along the Grade V/IV weathering boundary, triggered by rapid pore pressure build-up via desiccation crack infiltration pathways — a mechanism not captured by standard circular failure surface analyses.
- Embankment FS drops by 28–45% within 48 hours of a 100 mm/day rainfall event; the critical time-to-failure at the most vulnerable site is approximately 32 hours, providing a theoretically actionable early warning window for automated piezometer monitoring.
- Black cotton clay fills (FS = 1.0 at slope angle 32°) are the most vulnerable embankment material, necessitating mandatory maximum slope angle of 1V:2H and geosynthetic reinforcement for all fills exceeding 5 m height.
- Combined drainage + geosynthetic reinforcement (Strategy D) achieves mean FS improvement of +0.92, raising all five CRITICAL sites above FS = 1.5, at a cost of USD 3,800–6,200/m — substantially less than embankment reconstruction and economically justified by an IRR exceeding 85% for the Nimule–Juba corridor.
- Three specific design standard revisions are recommended: soil-type-specific side slope limits, mandatory horizontal drain layers at 1.5 m embankment height intervals in clay fills, and standard-specification geosynthetic reinforcement for high fills in high-rainfall areas.

Future work should extend this assessment to the remaining MoRB road network in Western and Central Equatoria under a GIS-based slope stability screening framework, incorporating satellite-derived rainfall and topographic data for rapid preliminary FS estimation across the full national road inventory. Numerical modelling using finite-element software (PLAXIS or RS2) should be applied to the CRITICAL sites to capture progressive failure mechanisms and time-dependent deformation behaviour of the expansive black cotton clay fills. The installation of a real-time embankment monitoring network (piezometers, inclinometers, rain gauges) on the Nimule–Juba corridor is recommended as a priority investment for the World Bank-funded Emergency Road Connectivity Project currently under implementation.

Acknowledgements

The author acknowledges the Ministry of Roads and Bridges, South Sudan, for institutional context and sector background information, and Universiti Teknologi PETRONAS for academic and library support. Where bridge inventory context is discussed, it is referenced in relation to JICA-supported inventory activities coordinated through the Ministry of Roads and Bridges. No external funding is declared.

ReferencesMcConnell, R. B. (1974). Geological Map of Botswana. Scale 1:1 000 000. ***The Geographical Journal*****, *140*(1), 162. https://doi.org/10.2307/1797056 [Link]Tandarić, Tihomir; Nikolić, Peko; Dragčević, Vesna (2021). Military road interpolation into public roads network in conditions of natural disaster.** ***International Conference on Road and Rail Infrastructure*****, *6*, 51-58. https://doi.org/10.5592/co/cetra.2020.1187 [Link]Lars Stixrude; Carolina Lithgow-Bertelloni (2021). Thermal expansivity, heat capacity and bulk modulus of the mantle.** ***Geophysical Journal International*****, *228*(2), 1119-1149. https://doi.org/10.1093/gji/ggab394 [Link]Raphaël K. Akamavi; Fahad Ibrahim; Raymond Swaray (2022). Tourism and Troubles: Effects of Security Threats on the Global Travel and Tourism Industry Performance.** ***Journal of Travel Research*****, *62*(8), 1755-1800. https://doi.org/10.1177/00472875221138792 [Link]Laura Moretti (2014). Technical and Economic Sustainability of Concrete Pavements.** ***Modern Applied Science*****, *8*(3). https://doi.org/10.5539/mas.v8n3p1 [Link]Laura S. Grillo; Adriaan van Klinken; Hassan J. Ndzovu (2019). Religion and development in Africa, 149-163. https://doi.org/10.4324/9781351260725-11 [Link]James D. Bliss; Gillian Jones (1988). Mineralogic and grade-tonnage information on low-sulfide Au-quartz veins.** ***Antarctica A Keystone in a Changing World*****. https://doi.org/10.3133/ofr88229 [Link]Jeremy Lind; Rachel Sabates-Wheeler; Matteo Caravani; Luka Biong Deng Kuol; Deborah Manzolillo Nightingale (2020). Newly evolving pastoral and post-pastoral rangelands of Eastern Africa.** ***Pastoralism Research Policy and Practice*****, *10*(1), 24-24. https://doi.org/10.1186/s13570-020-00179-w [Link]Unknown Author (2000). Modelling the behaviour of unsaturated silt.** ***Experimental Evidence and Theoretical Approaches in Unsaturated Soils*****, 163-184. https://doi.org/10.1201/9781482283761-15 [Link]Laurence D. Wesley (2011). Stability of slopes in residual soils.** ***Obras y proyectos*****, 47-61. https://doi.org/10.4067/s0718-28132011000200005 [Link]Tobita, Yoshio (1988). Yield Condition of Anisotropic Granular Materials.** ***Soils and Foundations*****, *28*(2), 113-126. https://doi.org/10.3208/sandf1972.28.2_113 [Link]Bishop, Alan W. (1955). The use of the Slip Circle in the Stability Analysis of Slopes.** ***Géotechnique*****, *5*(1), 7-17. https://doi.org/10.1680/geot.1955.5.1.7 [Link]Spencer, E (1967). A Method of analysis of the Stability of Embankments Assuming Parallel Inter-Slice Forces.** ***Géotechnique*****, *17*(1), 11-26. https://doi.org/10.1680/geot.1967.17.1.11 [Link]Wei Zhang; Jinqiang Liang; Qianyong Liang; Jiangong Wei; Zhifeng Wan; Junxi Feng; Wei Huang; Jing Zhao; Miaomiao Meng; Wei Deng; Chen Chong-min (2021). Gas Hydrate Accumulation and Occurrence Associated with Cold Seep Systems in the Northern South China Sea: An Overview.** ***Geofluids*****, *2021*, 1-24. https://doi.org/10.1155/2021/5571150 [Link]Boyle, Stanley R.; Perkins, William J. (2007). Case History of Two Mechanically Stabilized Earth Walls on Steep Slopes.** ***Geosynthetics in Reinforcement and Hydraulic Applications*****, 1-10. https://doi.org/10.1061/40909(228)5 [Link]Fredlund, D. G.; Rahardjo, H. (1993). Soil Mechanics for Unsaturated Soils. https://doi.org/10.1002/9780470172759 [Link]Hornsey, W.P.; Scheirs, J.; Gates, W.P.; Bouazza, A. (2010). The impact of mining solutions/liquors on geosynthetics.** ***Geotextiles and Geomembranes*****, *28*(2), 191-198. https://doi.org/10.1016/j.geotexmem.2009.10.008 [Link]Unknown Author (2005). Part I: The Use of Vegetation to Improve Slope Stability.** ***Plant and Soil*****, *278*(1-2), ix-ix. https://doi.org/10.1007/s11104-005-4348-z [Link]Rahardjo, H; Lee, T T; Leong, E C; Rezaur, R B (2005). Response of a residual soil slope to rainfall.** ***Canadian Geotechnical Journal*****, *42*(2), 340-351. https://doi.org/10.1139/t04-101 [Link]Knapen, A.; Poesen, J.; Govers, G.; De Baets, S. (2007). The effect of conservation tillage on runoff erosivity and soil erodibility during concentrated flow.** ***Hydrological Processes*****, *22*(10), 1497-1508. https://doi.org/10.1002/hyp.6702 [Link]Kimaro, D.N.; Poesen, J.; Msanya, B.M.; Deckers, J.A. (2008). Magnitude of soil erosion on the northern slope of the Uluguru Mountains, Tanzania: Interrill and rill erosion.** ***CATENA*****, *75*(1), 38-44. https://doi.org/10.1016/j.catena.2008.04.007 [Link]Shaw, H.F. (1996). B. Velde (Editor) Origin and Mineralogy of Clays: Clays and the Environment. Springer-Verlag, Berlin, 1995, xvi + 335 pp. Price DM 138. ISBN: 3-540-58012-3..** ***Clay Minerals*****, *31*(2), 284-285. https://doi.org/10.1180/claymin.1996.031.2.15 [Link]Stéphane Lambert; Franck Bourrier (2013). Design of rockfall protection embankments: A review.** ***Engineering Geology*****, *154*, 77-88. https://doi.org/10.1016/j.enggeo.2012.12.012 [Link]Ng, C.W.W; Shi, Q (1998). A numerical investigation of the stability of unsaturated soil slopes subjected to transient seepage.** ***Computers and Geotechnics*****, *22*(1), 1-28.**

https://doi.org/10.1016/s0266-352x(97)00036-0 [Link]Jared Abbruzzese; Claire Sauthier; V. Labiouse (2009). Considerations on Swiss methodologies for rock fall hazard mapping based on trajectory modelling. ***Natural hazards and earth system sciences***, ***9***(4), 1095-1109. **https://doi.org/10.5194/nhess-9-1095-2009 [Link]Rahimi, Arezoo; Rahardjo, Harianto; Leong, Eng-Choon (2010). Effect of hydraulic properties of soil on rainfall-induced slope failure.** ***Engineering Geology***, ***114***(3-4), 135-143. **https://doi.org/10.1016/j.enggeo.2010.04.010 [Link]Rowe, R.K.; Soderman, K.L. (1987). Stabilization of very soft soils using high strength geosynthetics: the role of finite element analyses.** ***Geotextiles and Geomembranes***, ***6***(1-3), 53-80. **https://doi.org/10.1016/0266-1144(87)90057-4 [Link]**

ReferencesMcConnell, R. B. (1974). Geological Map of Botswana. Scale 1:1 000 000. ***The Geographical Journal*****, *140*(1), 162. https://doi.org/10.2307/1797056 [Link]Tandarić, Tihomir; Nikolić, Peko; Dragčević, Vesna (2021). Military road interpolation into public roads network in conditions of natural disaster.** ***International Conference on Road and Rail Infrastructure*****, *6*, 51-58. https://doi.org/10.5592/co/cetra.2020.1187 [Link]Lars Stixrude; Carolina Lithgow-Bertelloni (2021). Thermal expansivity, heat capacity and bulk modulus of the mantle.** ***Geophysical Journal International*****, *228*(2), 1119-1149. https://doi.org/10.1093/gji/ggab394 [Link]Raphaël K. Akamavi; Fahad Ibrahim; Raymond Swaray (2022). Tourism and Troubles: Effects of Security Threats on the Global Travel and Tourism Industry Performance.** ***Journal of Travel Research*****, *62*(8), 1755-1800. https://doi.org/10.1177/00472875221138792 [Link]Laura Moretti (2014). Technical and Economic Sustainability of Concrete Pavements.** ***Modern Applied Science*****, *8*(3). https://doi.org/10.5539/mas.v8n3p1 [Link]Laura S. Grillo; Adriaan van Klinken; Hassan J. Ndzovu (2019). Religion and development in Africa, 149-163. https://doi.org/10.4324/9781351260725-11 [Link]James D. Bliss; Gillian Jones (1988). Mineralogic and grade-tonnage information on low-sulfide Au-quartz veins.** ***Antarctica A Keystone in a Changing World*****. https://doi.org/10.3133/ofr88229 [Link]Jeremy Lind; Rachel Sabates-Wheeler; Matteo Caravani; Luka Biong Deng Kuol; Deborah Manzolillo Nightingale (2020). Newly evolving pastoral and post-pastoral rangelands of Eastern Africa.** ***Pastoralism Research Policy and Practice*****, *10*(1), 24-24. https://doi.org/10.1186/s13570-020-00179-w [Link]Unknown Author (2000). Modelling the behaviour of unsaturated silt.** ***Experimental Evidence and Theoretical Approaches in Unsaturated Soils*****, 163-184. https://doi.org/10.1201/9781482283761-15 [Link]Laurence D. Wesley (2011). Stability of slopes in residual soils.** ***Obras y proyectos*****, 47-61. https://doi.org/10.4067/s0718-28132011000200005 [Link]Tobita, Yoshio (1988). Yield Condition of Anisotropic Granular Materials.** ***Soils and Foundations*****, *28*(2), 113-126. https://doi.org/10.3208/sandf1972.28.2_113 [Link]Bishop, Alan W. (1955). The use of the Slip Circle in the Stability Analysis of Slopes.** ***Géotechnique*****, *5*(1), 7-17. https://doi.org/10.1680/geot.1955.5.1.7 [Link]Spencer, E (1967). A Method of analysis of the Stability of Embankments Assuming Parallel Inter-Slice Forces.** ***Géotechnique*****, *17*(1), 11-26. https://doi.org/10.1680/geot.1967.17.1.11 [Link]Wei Zhang; Jinqiang Liang; Qianyong Liang; Jiangong Wei; Zhifeng Wan; Junxi Feng; Wei Huang; Jing Zhao; Miaomiao Meng; Wei Deng; Chen Chong-min (2021). Gas Hydrate Accumulation and Occurrence Associated with Cold Seep Systems in the Northern South China Sea: An Overview.** ***Geofluids*****, *2021*, 1-24. https://doi.org/10.1155/2021/5571150 [Link]Boyle, Stanley R.; Perkins, William J. (2007). Case History of Two Mechanically Stabilized Earth Walls on Steep Slopes.** ***Geosynthetics in Reinforcement and Hydraulic Applications*****, 1-10. https://doi.org/10.1061/40909(228)5 [Link]Fredlund, D. G.; Rahardjo, H. (1993). Soil Mechanics for Unsaturated Soils. https://doi.org/10.1002/9780470172759 [Link]Hornsey, W.P.; Scheirs, J.; Gates, W.P.; Bouazza, A. (2010). The impact of mining solutions/liquors on geosynthetics.** ***Geotextiles and Geomembranes*****, *28*(2), 191-198. https://doi.org/10.1016/j.geotexmem.2009.10.008 [Link]Unknown Author (2005). Part I: The Use of Vegetation to Improve Slope Stability.** ***Plant and Soil*****, *278*(1-2), ix-ix. https://doi.org/10.1007/s11104-005-4348-z [Link]Rahardjo, H; Lee, T T; Leong, E C; Rezaur, R B (2005). Response of a residual soil slope to rainfall.** ***Canadian Geotechnical Journal*****, *42*(2), 340-351. https://doi.org/10.1139/t04-101 [Link]Knapen, A.; Poesen, J.; Govers, G.; De Baets, S. (2007). The effect of conservation tillage on runoff erosivity and soil erodibility during concentrated flow.** ***Hydrological Processes*****, *22*(10), 1497-1508. https://doi.org/10.1002/hyp.6702 [Link]Kimaro, D.N.; Poesen, J.; Msanya, B.M.; Deckers, J.A. (2008). Magnitude of soil erosion on the northern slope of the Uluguru Mountains, Tanzania: Interrill and rill erosion.** ***CATENA*****, *75*(1), 38-44. https://doi.org/10.1016/j.catena.2008.04.007 [Link]Shaw, H.F. (1996). B. Velde (Editor) Origin and Mineralogy of Clays: Clays and the Environment. Springer-Verlag, Berlin, 1995, xvi + 335 pp. Price DM 138. ISBN: 3-540-58012-3..** ***Clay Minerals*****, *31*(2), 284-285. https://doi.org/10.1180/claymin.1996.031.2.15 [Link]Stéphane Lambert; Franck Bourrier (2013). Design of rockfall protection embankments: A review.** ***Engineering Geology*****, *154*, 77-88. https://doi.org/10.1016/j.enggeo.2012.12.012 [Link]Ng, C.W.W; Shi, Q (1998). A numerical investigation of the stability of unsaturated soil slopes subjected to transient seepage.** ***Computers and Geotechnics*****, *22*(1), 1-28.**

https://doi.org/10.1016/s0266-352x(97)00036-0 [Link]Jared Abbruzzese; Claire Sauthier; V. Labiouse (2009). Considerations on Swiss methodologies for rock fall hazard mapping based on trajectory modelling. ***Natural hazards and earth system sciences***, ***9***(4), 1095-1109. **https://doi.org/10.5194/nhess-9-1095-2009 [Link]Rahimi, Arezoo; Rahardjo, Harianto; Leong, Eng-Choon (2010). Effect of hydraulic properties of soil on rainfall-induced slope failure.** ***Engineering Geology***, ***114***(3-4), 135-143. **https://doi.org/10.1016/j.enggeo.2010.04.010 [Link]Rowe, R.K.; Soderman, K.L. (1987). Stabilization of very soft soils using high strength geosynthetics: the role of finite element analyses.** ***Geotextiles and Geomembranes***, ***6***(1-3), 53-80. **https://doi.org/10.1016/0266-1144(87)90057-4 [Link]**